Solid State Ionics 70/71 (1994) 465–470
North-Holland

SOLID STATE IONICS

EXAFS study of Nd^{3+}-exchanged β″-alumina crystal

F. Rocca
Centro CNR di Fisica degli Stati Aggregati ed Impianto Ionico, I-38050 Povo (Trento), Italy

A. Kuzmin, J. Purans
Institute of Solid State Physics, University of Latvia, LV-1063 Riga, Latvia

and

G. Mariotto
Dipartimento di Fisica, Università di Trento, I-38050 Povo (Trento), Italy

The local structure around the Nd^{3+} ions in 60%-exchanged sodium β″-alumina was studied by X-ray absorption spectroscopy. The analysis of the Nd L_3-edge experimental data shows that neodymium ions are mainly located near mid-oxygen (9d) sites. The local environment of Nd is slightly changed compared to crystallographic positions: the Nd–O(5) distance is shortened by 0.36 Å, while the Nd–Al(6c) is increased by 0.13 Å. The values of Debye–Waller factors of different coordination shells are discussed in terms of vibrational correlation.

1. Introduction

Sodium β″-alumina shows a great ability to incorporate by ion exchange reaction a variety of lanthanide ions in the conduction region between two spinel-blocks [1]. The exchanged compositions exhibit very interesting optical properties which make β″-alumina a very promising candidate for optoelectronic applications [2]. Recently, there has been a considerable interest for Nd^{3+}-exchanged β″-alumina crystals especially after obtaining lasing effects [3]. A combination of structural methods (X-ray diffraction (XRD) [4] and transmission electron microscopy (TEM) [5]), spectroscopic techniques (optical [6–8], electron paramagnetic resonance (EPR) [7] and X-ray absorption [9–11]) and molecular-dynamics simulations [11] has been used to probe the local environments of Nd^{3+} ions at different levels of ion exchange in the disordered lattice of the β″-alumina crystals. A schematic representation of the conduction region with possible neodymium sites is shown in fig. 1a. The Nd environment is strongly dependent on the ion content, and a better knowledge of the local structure is necessary.

X-ray absorption spectroscopy (XAS) provides additional information to XRD: in particular, the lattice distortion around the incorporated ions in crystalline materials can be studied by local point of view while, in contrast, XRD gives only average lattice structure. We have to notice too that for solid solutions there is some difference between the average lattice structure obtained by XRD and the local environment obtained by XAS of incorporated ions [12].

In this paper we report on the results of a detailed EXAFS study of the Nd L_3-absorption edge for a powdered Nd β″-alumina crystal (60%-exchanged by Nd).

2. Experimental

Single-crystal platelets of the β″-alumina, nominally $Na_{1.67}Mg_{0.67}Al_{10.33}O_{17}$, were grown by flux evaporation technique [13]. A 60% Nd^{3+}-exchanged sodium β″-alumina crystal was obtained by

0167-2738/94/$ 07.00

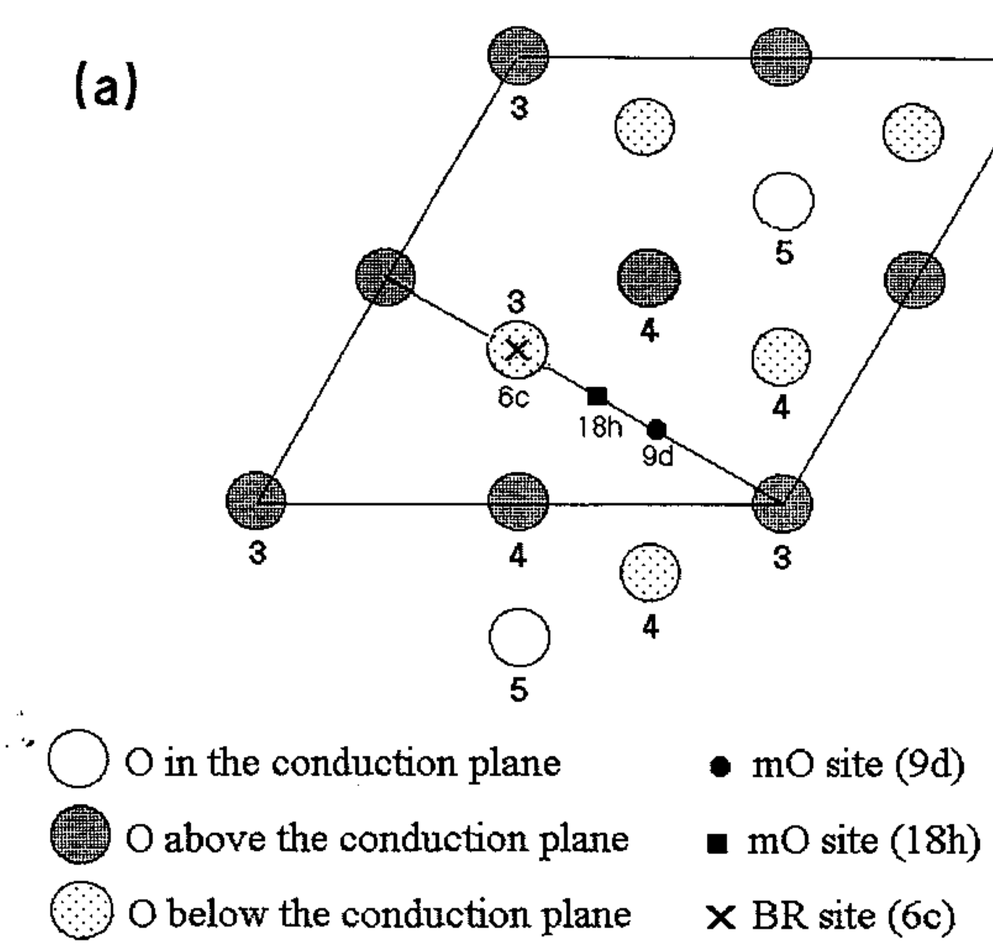

Fig. 1. (a) The conduction region in β″-alumina. The possible neodymium sites (mO (9d), mO (18h) and BR (6c)) are shown. (b) The structural model of the Nd environment determined in this work. The neodymium is located in the relaxed mO (9d) site.

remaining a platelet in molten $NdCl_3$ at 650°C for 24 h. The extent of exchange was measured by ^{22}Na radio-diffusion tracer technique [14].

The sample for EXAFS measurements was prepared as follows: the Nd^{3+}-exchanged sodium β″-alumina crystal was finely ground. The powder was dispersed in alcohol with an ultrasonic mixer and then slowly deposited on a polytetrafluoroethylene membrane.

The X-ray absorption spectra were measured in transmission mode at the ADONE storage ring (Frascati, Italy) using the EXAFS station on the PWA BX2S wiggler beam line. The electron energy was 1.5 GeV with current 10–40 mA. The synchrotron radiation was monochromatized using a Si(111) ($2d \simeq 6.271$ Å) channel-cut crystal monochromator, and its intensity was measured by two ionization chambers filled with krypton gas. Many experimental spectra were recorded at room temperature in the energy range 6100–6700 eV at the Nd L_3-edge ($E_{L_3} = 6207.9$ eV) with a 0.6–1.1 eV spacing and energy resolution equal to ~1 eV. The range of the L_3-edge EXAFS is limited by the presence of the neodymium L_2-edge ($E_{L_2} = 6721.5$ eV).

3. EXAFS data analysis

The experimental data were analyzed by the EXAFS Data Analysis "EDA" software package [15].

The X-ray absorption coefficient $\mu(E) = \ln(I_0/I)$ was obtained from the intensities of synchrotron radiation, measured by two ionization chambers, before (I_0) and after (I) the sample. The background contribution $\mu_b(E)$ was approximated by Victoreen rule and subtracted from the experimental spectrum $\mu(E)$. Further, the atomic-like contribution $\mu_0(E)$ was found by a combined polynomial/cubic-spline technique to have a precise removal of the EXAFS-signal zero-line, and the EXAFS-signal $\chi(E)$ was determined as $\chi(E) = (\mu - \mu_b - \mu_0)/\mu_0$. To convert $\chi(E)$ into a space of the photoelectron wavevector $k = \sqrt{(2m/\hbar^2)(E - E_0)}$ the energy origin E_0 was set at 3.2 eV above the white line maximum according to the procedure utilized by us earlier [16]. The EXAFS-signal $\chi(k)$ was multiplied by a factor k^2 to compensate the decrease of its amplitude with the increase of the wavevector value (see dotted curve in fig. 2a).

The Fourier transform (FT) with a Gaussian window of the experimental EXAFS-signal in the range from 1.0 to 10.0 $Å^{-1}$ is shown in fig. 2b. There are two main well visible peaks located at 2 and 3 Å and some broad less intense peaks at 4 and 5.4 Å. The low intensity signal of FT above 6 Å means that the noise in the experimental spectrum, shown in fig. 2a, has a "white" character.

The contribution (solid curve in fig. 2a) to the total EXAFS-signal from the first two well visible peaks in fig. 2b was singled out by the back FT in the range 0.9–3.5 Å. The difference between signals derived from independent measurements was less than 6%.

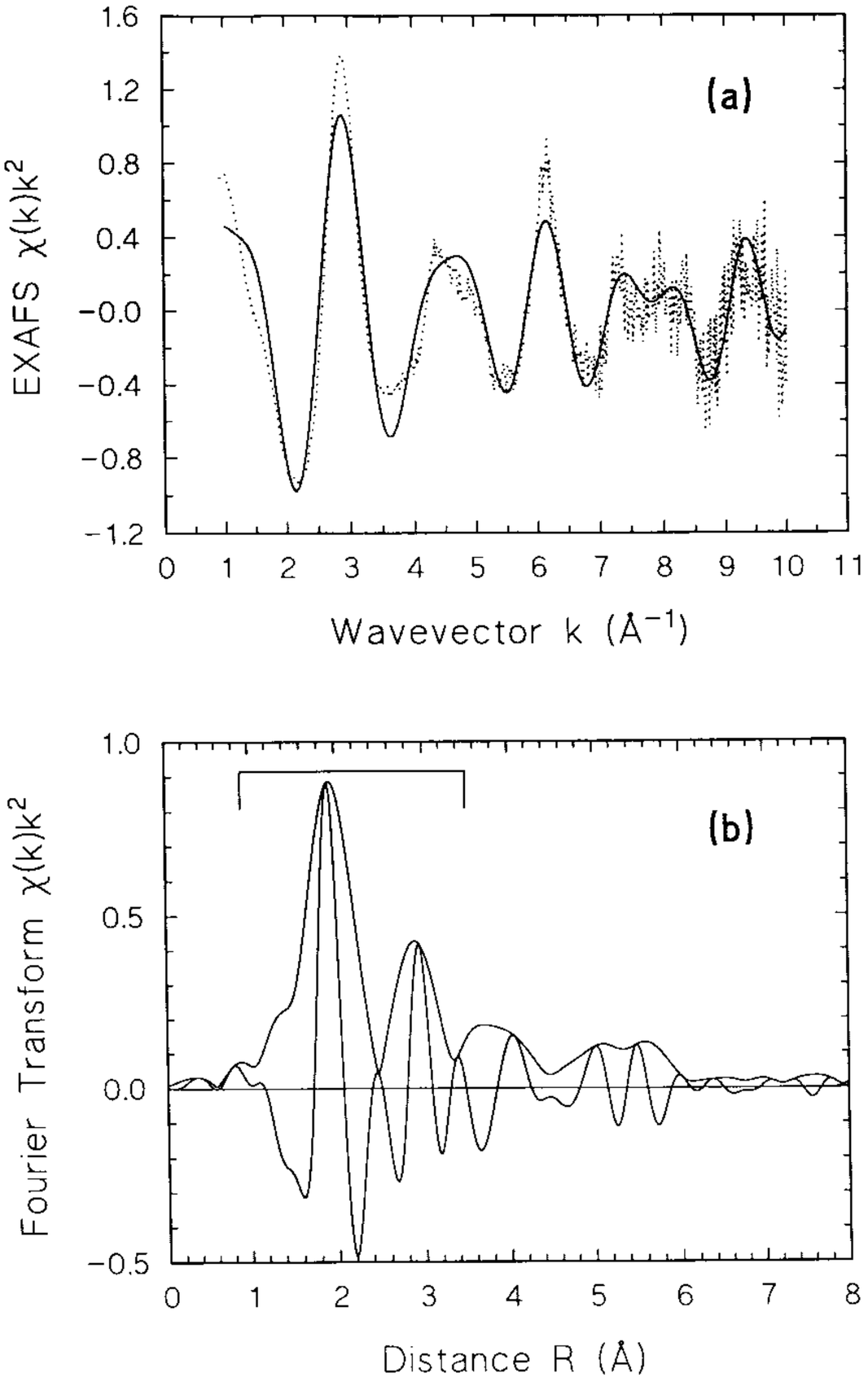

Fig. 2. (a) Experimental EXAFS $\chi(k)k^2$ of the Nd L_3-edge (dotted line) and the contribution from the first two peaks (see (b)) singled out by the back FT in the range 0.9–3.5 Å (solid line). (b) Fourier transform of the experimental EXAFS $\chi(k)k^2$ spectrum. The range of the back FT is indicated.

The obtained $\chi(k)k^2$ signal ($k=1.0$–10.0 Å^{-1}) was utilized in the best fit multi-shells analysis procedure.

The calculations of the EXAFS function were based on the single-scattering curved-wave formalism [17,18] which is the only expected contribution to the first two peaks in the range 0.9–3.5 Å (fig. 2b). The EXAFS $\chi(k)$ was calculated using the expression

$$\chi(k)=\sum_i \frac{N_i}{kR_i^2} f_i(k, R_i)\exp(-2\sigma_i^2 k^2) \times \sin[2kR_i+\phi_i(k, R_i)] ,$$

where N_i is the coordination number of the i-shell, R_i is the radius of the i-shell, σ_i is the Debye–Waller factor, $f_i(k, R_i)$ is the backscattering amplitude of the photoelectron by atoms of i-coordination shell, $\phi_i(k, R_i)$ is the phase shift of the photoelectron determined by central and scattering atoms. The backscattering amplitudes $f_i(k, R_i)$ and phases $\phi_i(k, R_i)$ were previously calculated by the FEFF3 code [19,20] for Nd–O pair ($R=2.5$ Å) and Nd–Al pair ($R=3.5$ Å). The parameters of calculations were optimized by comparison with $NdCoO_3$ and $NdNiO_3$ reference compounds.

The result of the fitting procedure gives us the set of structural parameters presented in table 1. There are two shells which produce the main contribution to the EXAFS-signal: a group of oxygen atoms centered at 2.46 ± 0.02 Å and a group of aluminum atoms centered at 3.35 ± 0.03 Å. The two-shells model allows to approximate the general behaviour of the EXAFS-signal, but large disagreement with experiment remains at high k-values (7.5–9 Å^{-1}). To achieve better agreement between theory and experiment, it is necessary to take into account two more shells. The addition of the second oxygen shell at 2.66 ± 0.04 Å improves the agreement of the first peak in FT while the third oxygen shell at 3.8 ± 0.1 Å improves the best fit to the second peak. Thus, using a four-shells model, it is possible to describe the shape of the experimental signal enough precisely in all energy range from 1.5 to 9.0 Å^{-1}.

4. Discussion

It was suggested by single-crystal room-temperature X-ray diffraction studies [4] that Nd^{3+} ions at high level of exchange exhibit a strong preference for the mid-oxygen (mO) (9d) site (95%) where they are strongly coordinated to two very short ($R\approx2.46$

Table 1
Structural data obtained from the analysis of the Nd L_3-edge EXAFS. (N is the number of atoms A located at the distance R from neodymium, σ^2 is the Debye–Waller factor.)

A	N	R (Å)	σ^2 (Å^2)
O	2.3 ± 0.5	2.46 ± 0.02	0.001 ± 0.001
O	5.1 ± 0.5	2.66 ± 0.04	0.025 ± 0.010
Al	3.2 ± 0.9	3.35 ± 0.03	0.003 ± 0.002
O	2.44 ± 1.0	3.8 ± 0.1	0.02 ± 0.015

Å) relaxed oxygen O(5) neighbours in the conduction region and six oxygen neighbours ($R \approx 2.70$ Å) located at the spinel-blocks. The remainder 5% of neodymium ions were found in alternate tetragonal Beever–Ross (BR) sites (6c). The Nd^{3+}-exchange process causes a shortening of the *c*-axis and a narrowing of the conduction slabs. The average electron distribution map shows a high anisotropy of the neodymium vibrations in the conduction region in the direction along the "conduction pathways" [4].

The general agreement between our data (table 1) and XRD (table 2 in ref. [4]) is quite good. It is necessary to point out that the content of neodymium in our sample is smaller: this can be one of the reasons of some difference in the values of structural parameters.

Now we want to compare our results with local structure around possible crystallographic sites of neodymium in β″-alumina refined from XRD data [4]. There are three main positions where the Nd ions are supposed to be located: (i) mid-oxygen (mO) site (9d), (ii) mid-oxygen site (18h) and (iii) Beever–Ross (BR) site (6c). The comparison between pair radial distribution function (RDF) for each possible neodymium site from ref. [4] and RDF calculated from the EXAFS data is shown in fig. 3. The distribution of distances in the first shell is very wide in the case of the BR (6c) site (one short and six long distances), and it becomes more narrow during the transition to mO (18h) and mO (9d) sites. The second shell shows the opposite behaviour. It is well defined in the case of the BR (6c) site, becomes very broadened for the mO (18h) site and splits into two subshells for the mO (9d) site. In the last case two subshells have very well defined origin: the first one consists only of aluminum atoms and the second one is formed only by oxygens.

We performed a best fit analysis by modifying the local arrangement around Nd ions in each single possible site. The best agreement between the obtained radial distribution and modified structural models is achieved for the mO (9d) site. In this case, only the small shifts from crystallographic data of outer aluminum ($\Delta \sim 0.2$ Å) and oxygen ($\Delta \sim -0.1$ Å) shells are necessary. For the mO (18h) site the agreement is worse since a shift of oxygen ions ($\Delta \sim 0.2$ Å) in the first shell is required and the broadened distribution of distances above 3 Å is inconsistent with

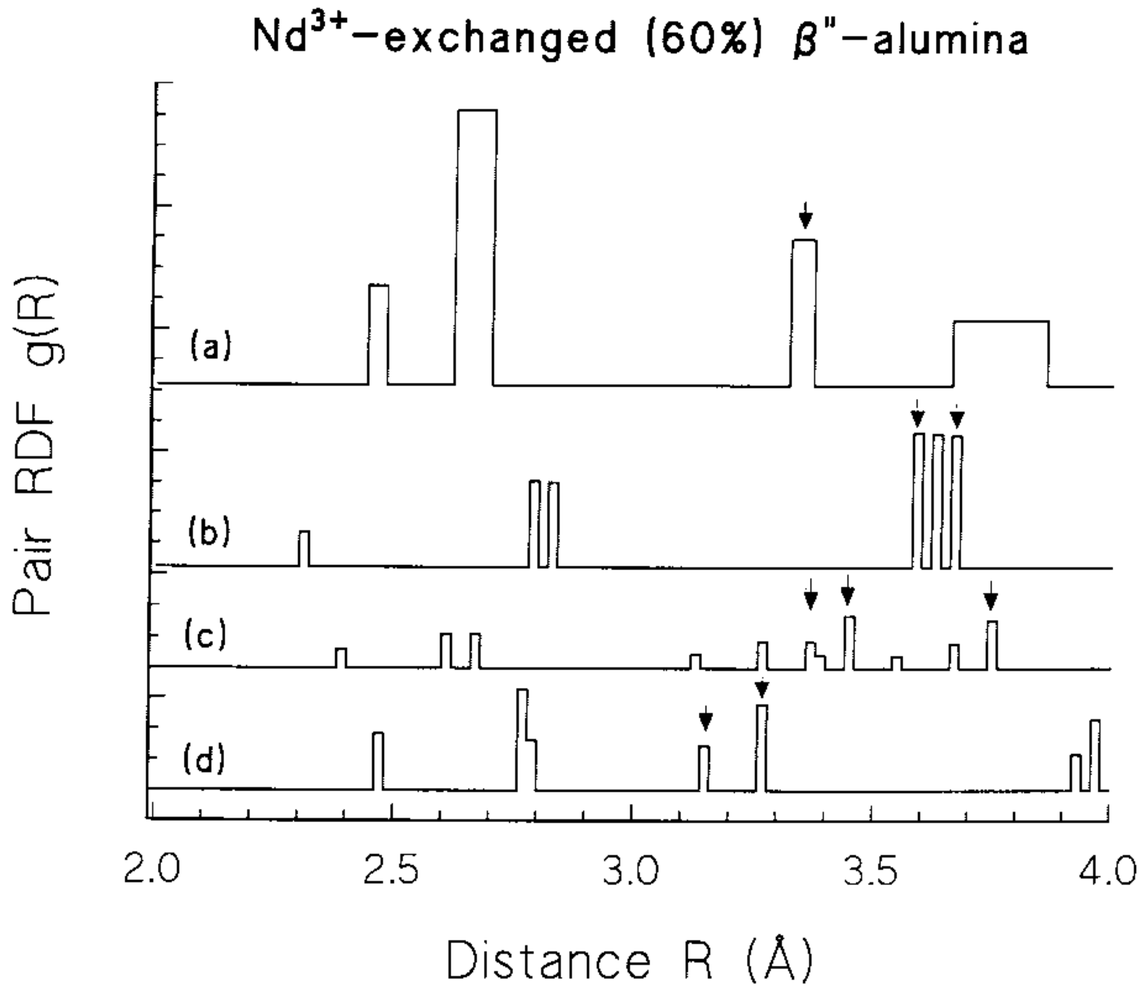

Fig. 3. Pair radial distribution functions (RDF) $g(R)$ for three crystallographic positions [4] ((b) Beever–Ross (6c), (c) mid-oxygen (mO) (18h) and (d) mO (9d)) of neodymium in β″-alumina in comparison with structural data obtained from EXAFS (a) in this work. The arrows indicate the peaks of aluminum subshells.

the well defined shape of the second peak in FT of EXAFS-signal. In the case of the BR (6c) site, the disagreement becomes the largest. Here, it would be necessary to relax all distances and, in addition, there is a big "problem" in the first coordination shell: the short distance (~ 2.2–2.3 Å) is absent in the EXAFS results, and, when one tries to improve the agreement by shifting the neodymium ion along *z*-axis (i.e. if we assume the off-center position of neodymium), the four shortest distances become ~ 2.46 Å, but the second contribution in the first coordination shell (oxygens at ~ 2.66 Å) disappears. A similar shift along the *z*-axis in the case of mO (18h) or mO (9d) sites does not change their agreement with obtained results. Besides the best fit multi-shell modelling with 3 free parameters (N, R, σ^2) in each shell described in section 3, the best fits starting from mO (9d), mO (18h) and BR (6c) positions were performed with coordination numbers fixed to their crystallographic values. The variation of distances were allowed within the interval ± 0.3 Å from their crystallographic values to simulate possible small relaxations, and the Debye–Waller factors σ^2 were free parameters. The obtained results agree with previous conclusions: the mO (9d) site allows to achieve the best

agreement with smaller required relaxations and the relaxations in the case of the BR (6c) site are the largest. Thus, the mO (9d) site with two short (~2.46 Å) Nd–O bonds in conduction region and about six long Nd–O bonds with oxygens above and below conduction region seems preferable from the analysis of EXAFS data.

Additional information, besides that from the distances and coordination numbers, can be obtained from the values of the Debye–Waller factors. We realize that in such a complicated structure as β″-alumina, having too short (from 1.5 to 9.0 $Å^{-1}$) and relatively noisy EXAFS spectrum, the absolute values of the Debye–Waller factors have more qualitative than quantitative character, nevertheless their relative values can be interpreted. There are two shells with the Debye–Waller factors significantly smaller than others (table 1): the first shell formed by two O(5) oxygens located at ~2.46 Å in the conduction region and the third shell formed by four aluminum atoms located at ~3.35 Å in the spinel-blocks above and below the O(5) bridging oxygens.

The large distance of aluminum atoms and the small value of Debye–Waller factor suggest that the Al-thermal motion is highly correlated with the neodymium one. The second oxygen shell located at ~2.66 Å has the value of the Debye–Waller factor much greater than the previous two shells. This cannot be explained by the static disorder: in fact, two crystallographic subshells at 2.69 and 2.72 Å give the contribution to the Debye–Waller factor only about 0.001 $Å^2$ that is much smaller than the estimated value 0.025 ± 0.010 $Å^2$. This suggests that contrary to the first case, the movements of these groups of oxygens are not correlated with that of neodymium.

5. Summary and conclusions

In this work we present a detailed analysis of the neodymium L_3-edge X-ray absorption spectrum of a powdered 60%-exchanged sodium β″-alumina crystal measured in transmission mode at room temperature.

On the basis of the EXAFS spectra analysis we can propose the following model of the neodymium local environment in 60% exchanged sodium β″-alumina (fig. 1b): the neodymium ions are located mainly near the mO (9d) site of the conduction region; they are strongly bonded to two O(5) oxygens which are located in the same plane and shifted from their crystallographic positions in pure sodium β″-alumina. Thus, the Nd–O(5) distance becomes about 0.36 Å shorter. The shift of the O(5) atoms leads to relaxation of four aluminum (Al(6c)) atoms in the opposite direction, so that the Nd–Al(6c) bond length becomes ~0.13 Å longer. The six oxygens located above and below the conduction region relax ~0.1 Å in the direction to neodymium. The thermal motion of neodymium, two oxygens (O(5)) and four aluminums (Al(6)) is highly correlated whereas there is no evidence of correlation between the neodymium ions and oxygens of the spinel-blocks.

Acknowledgement

The authors are indebted to Prof. P.K. Davies for kindly providing them with the crystal. They are also thankful to Dr. F. Tietz (Universität Hannover) for fruitful discussions and critical reading of the manuscript. A.K. and J.P. wish to thank the Università di Trento, Consiglio Nazionale delle Ricerche and INFN (Laboratori Nazionali di Frascati) for hospitality and financial support. They are especially grateful to the groups of Prof. G. Dalba (Università di Trento) and Prof. E. Burattini (Laboratori Nazionali di Frascati). This work has been partially supported by the Italian Consiglio Nazionale delle Ricerche No. 93-01312.CTO2.

References

[1] J.P. Boilot, G. Collin, Ph. Colomban and R. Comes, Phys. Rev. B 22 (1980) 5912.
[2] G.C. Farrington, B. Dunn and J.O. Thomas, Appl. Phys. A 32 (1983) 159.
[3] M. Jansen, A.J. Alfrey, O.M. Stafsudd, D.L. Yang, B. Dunn and G.C. Farrington, Opt. Lett. 9 (1984) 119.
[4] W. Carrillo-Cabrera, J.O. Thomas and G.C. Farrington, Solid State Ionics 28–30 (1988) 317.
[5] P.K. Davies, A. Petford and M. O'Keeffe, Solid State Ionics 18/19 (1986) 624.
[6] A.J. Alfrey, O.M. Stafsudd, B. Dunn and D.L. Yang, J. Chem. Phys. 88 (1988) 707.
[7] B. Dunn, D.L. Yang and D. Vivien, J. Solid State Chem. 73 (1988) 235.

[8] H. Dai and O.M. Stafsudd, J. Phys. Chem. Solids 52 (1991) 367.
[9] R. Wong, W.L. Roth, B. Dunn and D.L. Yang, Solid State Ionics 18/19 (1986) 599.
[10] M.L. denBoer, Y.S. Pak, K.J. Adamic, S.G. Greenbaum, M.C. Wintersgill, J.F. Lomax, J.J. Fontanella, B. Dunn and G.C. Farrington, Phys. Rev. B 45 (1992) 6369.
[11] T.S. Bush, C.R.A. Catlow, A.V. Chadwick, M. Cole, R.M. Geatches, G.N. Greaves and S.M. Tomlinson, J. Mater. Chem. 2 (3) (1992) 309.
[12] T. Yokoyama, F. Takamatsu, K. Seki, K. Miyake, T. Tani and T. Ohta, Japan. J. Appl. Phys. 29 (1990) L1486.
[13] J.L. Briant and G.C. Farrington, J. Solid State Chem. 33 (1980) 385.
[14] R.B. Queeman, Ph.D. Thesis (University of Pennsylvania, 1989).
[15] A. Kuzmin, unpublished.
[16] A. Kuzmin, J. Purans, M. Benfatto and C.R. Natoli, Phys. Rev. B 47 (1993) 2480.
[17] W.L. Schaich, Phys. Rev. B 14 (1976) 4420.
[18] S.J. Gurnman, N. Binsted and I. Ross, J. Phys. C 17 (1984) 143.
[19] J.J. Rehr, J. Mustre de Leon, S.I. Zabinsky and R.C. Albers, J. Am. Chem. Soc. 113 (1991) 5135.
[20] J. Mustre de Leon, J.J. Rehr, S.I. Zabinsky and R.C. Albers, Phys. Rev. B 44 (1991) 4146.